



ISSN: 0067-2904

Synthesis of Graphene Oxide Nanoparticles by Laser Ablation System

Atiaf K. Jeryo*, Qusay Adnan Abbas

Department of Physics, College of Science, University of Baghdad, Baghdad, Iraq

Received: 14/9/2019

Accepted: 17/12/2019

Abstract

In this study, graphene oxide (GO) and reduced graphene oxide were synthesized by pulsed Nd:YAG laser with a fundamental wavelength (1064 nm) focused on the pure graphite target which was immersed in distilled water. Different pulse energies were applied in two cases; with and without magnetic field. The synthesized GO and rGO nanoparticles were characterized by UV-visible spectroscopy, X-ray diffraction (XRD), Fourier transform infrared (FTIR) spectroscopy and atomic force microscopy (AFM) with and without magnetic field. The data show the presence of a magnetic field which illustrated increasing oxygen functional groups of GO. This caused a change in the morphology of the surface of GO, increasing crystallite size from 12.19 nm to 71.2 nm. The interlayer distance (d-space) was reduced from 0.4 nm to 0.25 nm and the absorption peaks that appeared in the spectrum were reduced and shifted toward smallest wavelengths, while the stretching vibration of the O-H group peak was shifted toward largest wavelengths.

Keywords: Graphene Oxide, Reduced Graphene Oxide, Laser Ablation, XRD, AFM, UV-Visible, FTIR.

تحضير جسيمات اوكسيد الكرافين النانوية بواسطة النظام الاستئصال بالليزر

اطياف خير الله جريو*, قصي عدنان عباس

قسم الفيزياء، كلية العلوم، جامعة بغداد، بغداد، العراق

الخلاصة

في هذه الدراسة تم تصنيع أكسيد الجرافين (GO) وتقليل أكسيد الجرافين (rGO) بواسطة ليزر النبضي Nd:YAG و بطول موجي 1064 نانومتر والذي تم تركزه على هدف الكرافيت النقي المغمور في الماء المقطر وعند طاقات نبضية مختلفة في حالة وجود وعدم وجود مجال مغناطيسي. حيث تم تشخيص جسيمات GO و rGO النانوية المركبة بواسطة التحليل الطيفي للأشعة فوق البنفسجية، حيود الأشعة السينية (XRD)، التحليل الطيفي للأشعة تحت الحمراء لتحويل فورييه (FTIR) وتحليل المجهرى للقوة الذرية (AFM) عند وجود وعدم وجود المجال المغناطيسي. فقد بينت البيانات، في حالة تسليط مجال مغناطيسي فإن نسبة مجاميع الاوكسجين سوف تزداد، تغير في مورفولوجية السطح لاوكسيد الكرافين، حجم البلوريسوف يزداد من 12.19 nm الى 71.2 nm، المسافة البينية سوف تقل من 0.4 nm الى 0.25 nm و ان قمة الامتصاص التي تظهر بالطيف سوف تقل وتتراج باتجاه الطول الموجي القليل بينما اصرة الممتدة للاهتزاز O-H سوف تتراج باتجاه الطول الموجي الطويل.

*Email: Ateafkhj94@gmail.com

1. Introduction

Carbon element represents one of the most common atoms on Earth, occurring naturally in many forms and as a component in innumerable substances which are called allotropes of carbon [1]. Graphene is one atomic thick sheet of sp^2 bonded carbon atoms including hexagonal lattice arrays [2-4]. Graphene is known as the thinnest, lightest and a very strong material. The thorough application of graphene is attributed to its chemical stability, high surface area, and excellent electrical, mechanical and thermal properties. Graphene applications include water purification, biosensors, drug delivery and nanocomposites [2,3,5,6].

Graphene is generated by the reduction process of graphene oxide (GO) that contains reactive oxygen functional groups such as carboxy, epoxides and alcohols, with a carbon to oxygen ratio of approximately three to one [3,7]. The reduced graphene oxide (rGO) can be produced by the reduction of GO by thermal [8], electrochemical [9] or chemical [10] processes.

GO can be produced by oxidizing graphite to interlard the carbon layers with oxygen molecules, and then few layers of graphene are produced by disuniting carbon atom layers completely by reducing graphite oxide [11]. GO is often described as an electrical insulator, similar to graphite oxide, because of the disruption of its sp^2 bonding networks. The amount of oxidization in the compound of GO and the method of synthesis determine the ability for GO to conduct electrons. The electrical conductivity of GO is disturbed by its oxidization in the solution, where the highly oxidized GO is caused to be a very poor electrical conductor. Even if GO were to be heavily reduced, though it would possibly be able to conduct electricity, it would still not perform as well as high quality graphene monolayers in terms of electron mobility [1]. Graphene oxide can be exfoliated into monolayers and this fact represents a difference between graphene oxide and graphite oxide. In addition, GO can be transformed to graphite oxide by many different techniques such as thermal, mechanical and various chemical processes [3,7].

GO is completely a byproduct of this oxidation, as when the oxidizing agents react with graphite, the inter planar spacing between the graphite layers is increased. Thereafter, the completely oxidized compound can be scattered in a base solution such as water, and then graphene oxide is generated [11]. The properties and structure of GO depend on the preparation method and degree of oxidation [1]. GO has recently appeared as a new carbon - based nano-scale material that furnishes an reciprocal path to graphene. Graphene oxide is a single-atomic-layered material made by oxidizing graphite crystals which are present in large quantities at inexpensive prices. The structure of GO is similar to a graphene sheet, with its base having oxygen-containing groups. Since these oxygen groups have a high relation with water molecules, it is hydrophilic and can be easily melted in water and other solvents. This allows it to be uniformly deposited onto substrates in the form of thin films or networks, which makes it potentially useful for microelectronics. Practically, the presence of oxygen groups in the structure of GO makes it a poor conductor, but most of graphene's properties are restored when it undergoes chemical, thermal or light reduction treatments. Commercially, GO represents one of the most available graphene materials. The basal planes and GO edges are functionalizing with exogenous groups, such as hydroxyl, epoxy, and carbonyl groups, which are attached at the edge [12]. Then, oxygen-containing functional groups disrupt the aromatic regions in the basal plane. Therefore, the GO layer consists of both aromatic regions and oxidized aliphatic six-membered rings, which causes to pervert SP^3 - hybridized geometry and results in the insulating property of GO. Industrially, there are a wide range of applications of GO, such as hydrogen storage and solar cells [13], paper like materials [14], transparent conductive films [15] nano electro mechanical devices [16], polymer composites [17] and biomedicine [18]. Moreover, other numerous GO applications have already been explored, such as biosensing [19], photocatalysis [20], electronics and optoelectronics [21].

The aim of this study is to synthesize GO rGO using laser ablation at atmospheric pressure with different pulsed laser energies. The synthesized materials were characterized using Fourier transform infrared spectroscopy (FTIR), x-ray diffractometer (XRD), UV-Visible spectrometer and Atomic Force Spectroscopy (AFM).

2. Experimental Setup

GO nanoparticles were synthesized by laser ablation of a high purity graphite target with distilled water, as shown in figure (1). The graphite target was first washed in an ultrasonic bath with deionized water to remove organic compounds and then placed at the bottom of a glass vessel containing 3ml of distilled water. Height of water on the graphite target was 2mm. A pulsed Nd:YAG laser with a

fundamental wavelength of 1064 nm and a repetition rate of 6Hz at different pulse laser energy (500, 600 and 700mJ) with and without magnetic field was used for the synthesis of graphene nanoparticles in distilled water with 500 pulse of the graphite target. One permanent magnet which has a value of 4.4mT was used to apply the magnetic field.

3. Characterization of Synthesized Graphene Oxide Nanoparticles

Several experimental methods are available to characterize the synthesized GO. The absorption spectrum of GO was recorded by using UV-Vis spectrophotometer [Shimadzu model) over a wavelength range of 190-1100nm. The size and morphology of GO nanoparticles were characterized by AFM (Angstrom advanced SPM-A 3000 model) and the presence of elemental GO, in the presence and absence of the magnetic field, was confirmed through X-ray diffraction (SHIMADZ XRD 600C) analysis with Cu- α x-ray tube ($\lambda=1.5418\text{\AA}$, $V=40\text{kV}$, $I=30\text{mA}$). The interaction between distilled water and graphene nanoparticles was analyzed by Fourier transforms infrared spectroscopy (FTIR) (SHIMADZU), which provides a record of absorption of electromagnetic radiation by sample in a wavenumber range of $400\text{-}4000\text{cm}^{-1}$.

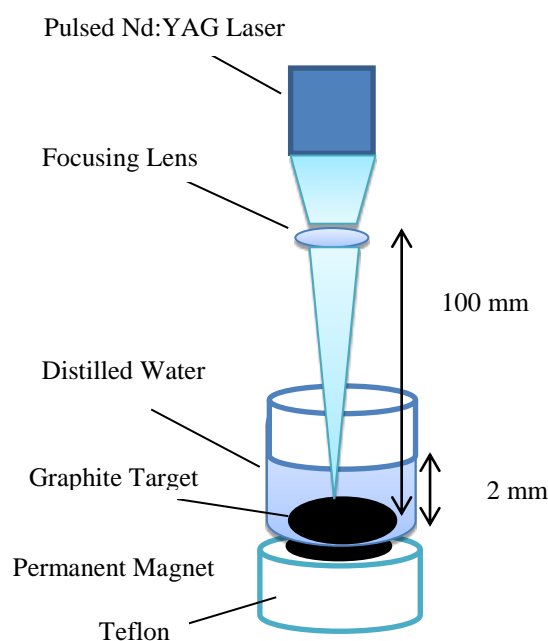


Figure 1-Experimental set up of laser ablation system.

2. Ultraviolet Visible Spectroscopy Analysis (UV-Visible)

The influence of laser energy on the absorption spectrum of GO nanoparticles in distilled water, in two cases of with and without magnetic field, was diagnosed by UV-VIS spectrophotometer. Figure -2 illustrates the influence of laser energy on the measurement of absorbance versus wavelength with and without magnetic field. The absorbance of GO nanoparticles was measured in the UV-Visible region (190-500nm).

Figure (2A) shows that when the laser energy is 500 mJ, the absorption peak at 221nm corresponds to the $\pi \rightarrow \pi^*$ transition of $C = C$ bonds [2]. When the laser energy was increased to 600mJ, the absorption peak was shifted from 221 to 209nm, while when laser energy was increased to 700mJ, the absorption peak remained at 221nm. The intensity of peaks related to oxygen functional groups of the GO were increased dramatically with increasing laser energy from 500 to 600mJ. This result may be attributed to the increase of oxygen functional groups of GO. When the laser energy was increased to 700mJ, the intensity of peaks related to oxygen functional groups of GO was reduced dramatically. These results imply a successful reduction of oxygen functional groups of GO.

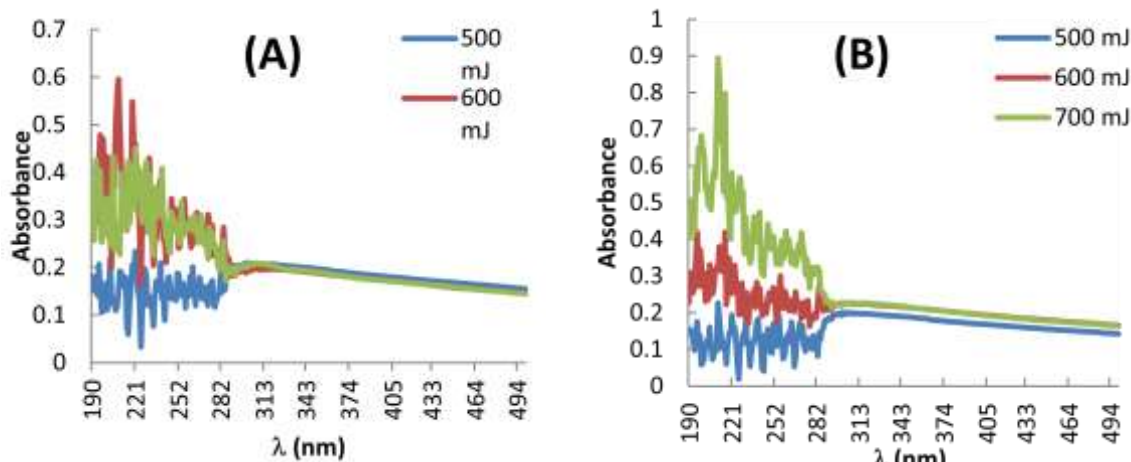


Figure 2-The FFFFof laser energy on absorption spectra of graphene nanoparticles in A) Absence of magnetic field and B) Presence of magnetic field.

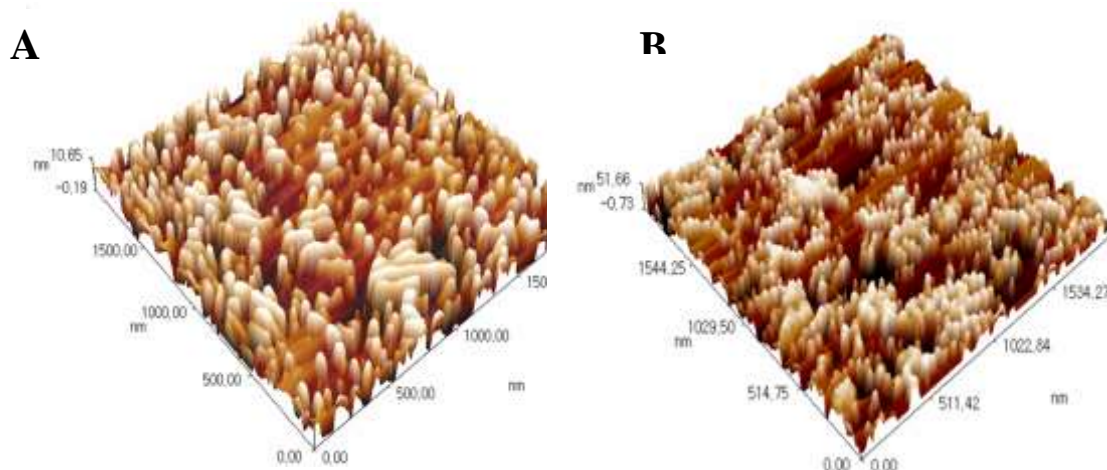
Figure-(2B) demonstrates that when the laser energy is increased, the absorption peak appears at 211nm during the application of the magnetic field. The absorption peak was shifted to 216nm with increasing laser energy from 500 to 600mJ. With further increasing laser energy from 600 to 700mJ, the absorption peak was reduced to become 211nm. This behavior is attributed to the reduction reaction and the formation of oxygen functional groups of GO.

The intensity of peaks was increased with increasing laser energy. This result indicates the increase of oxygen functional groups of GO in the presence of a magnetic field.

3. Atomic Force Microscope Analysis (AFM)

Figures-(3, 4) illustrate the atomic force microscopy images of GO produced by laser with different energy levels and 5 mg of graphite target in 3ml of distilled water, in both cases of with and without magnetic field.

It is clear from Figure-3 that the average thickness values of GO prepared with laser energy levels of 500, 600 and 700 mJ were 10.65, 51.66 and 25.95nm, respectively. On the other hand, the AFM images of GO nanoparticles in the presence of magnetic field show that the average thickness of GO layer was increasing with increasing laser energy; the average thickness values were 12.02, 12.43 and 30.51nm corresponding with laser energy levels of 500, 600 and 700mJ , respectively. The increase of the average thickness may be due to restocking of GO particles [2]. The comparison of Figures- (3) and (4) show that the presence of the magnetic field caused a change in the morphology of the surface. The values of average diameter and roughness of GO in the presence and absence of magnetic field are tabulated in



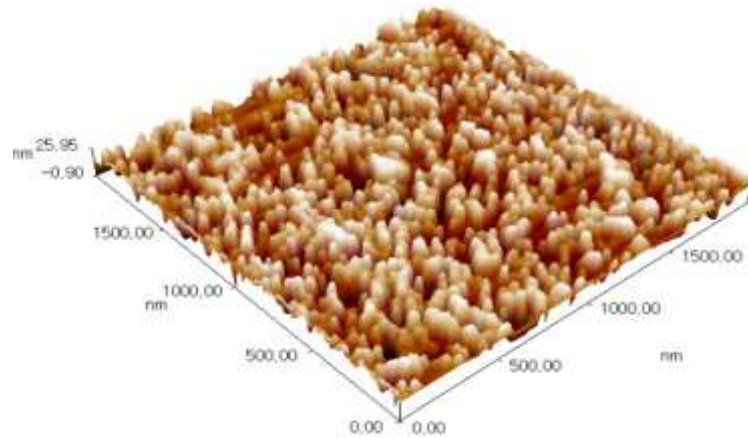


Figure 3-AFM images of graphene oxide that prepared at different laser energy; A) 500mJ, B) 600mJ and C) 700mJ without magnetic field

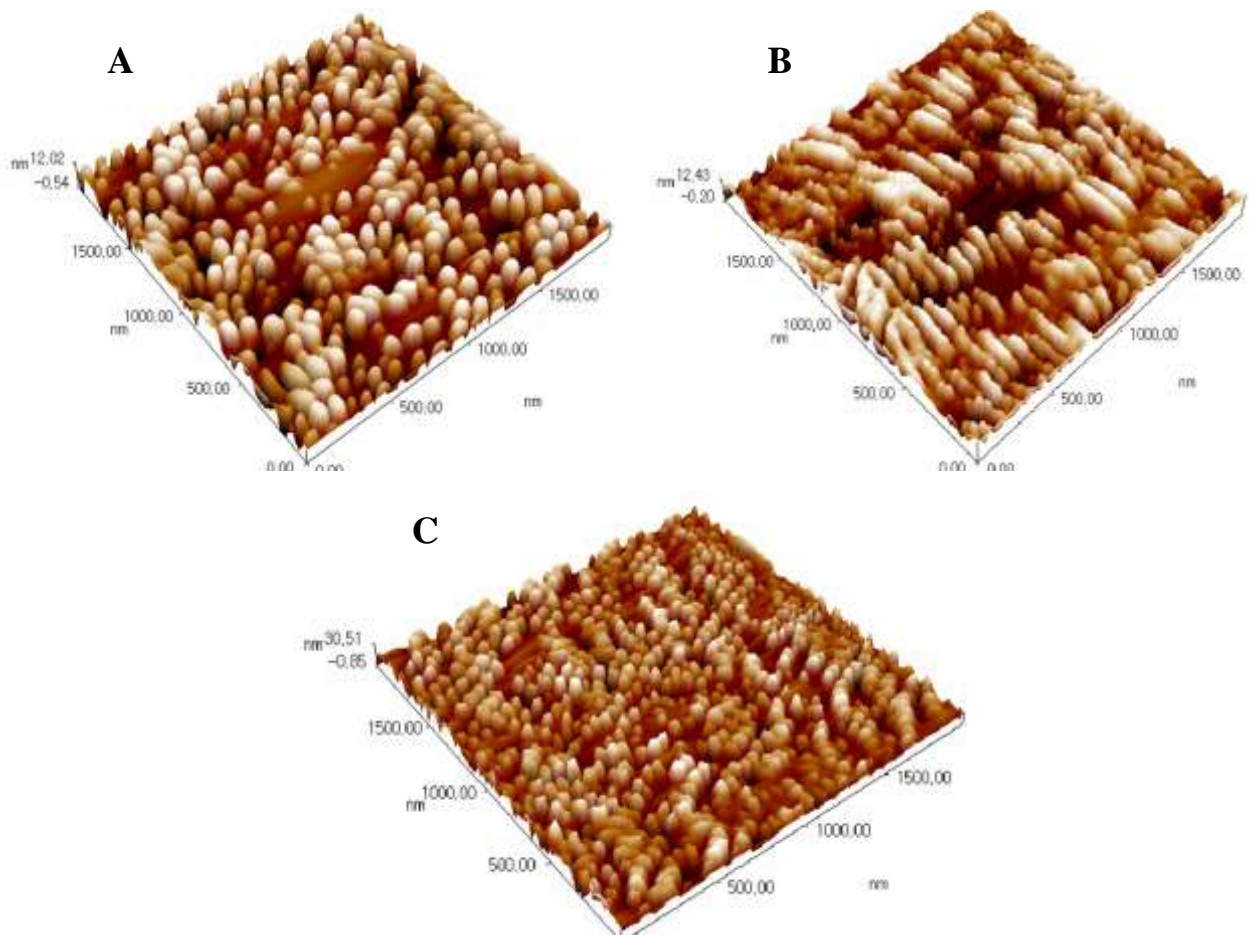


Figure 4-AFM images of graphene oxide prepared at different laser energy levels; A) 500mJ, B) 600mJ and C) 700mJ, with magnetic field.

Table 1-The average diameter and roughness average of GO prepared at different laser energy with and without magnetic field.

Without Magnetic Field		
Laser Energy (mJ)	Average Diameter (nm)	Roughness Average (nm)
500	71.88	2.71
600	65.2	13.1
700	57.07	5.9
With Magnetic Field		
500	80.06	3.14
600	69.35	2.84
700	59.43	5.9

This table indicates that the average diameters of GO particles were decreased with increasing laser energy in the presence and absence of magnetic field. The presence of magnetic field causes to increase the average diameter of GO particles in all laser energy levels. In addition, the roughness average of GO surface showed a different behavior with different laser energy levels in the presence and absence of the magnetic field. When the magnetic field was not applied and the laser energy was increased from 500 to 600mJ, the roughness average was increased from 2.71 to 13.1nm. The further increase in the laser energy from 600 to 700mJ caused the roughness to be reduced from 13.1 to 5.9nm. With the existence of magnetic field, when the laser energy was increased from 500 to 600mJ, the roughness average was decreased from 3.14 to 2.84nm. The further increase in the laser energy from 600 to 700mJ caused an increase in the roughness average from 2.84 to 5.9 nm. The surface roughness of the prepared films is attributed to the degree of material oxidation, because of the greater oxidation degree will be at spaced more functional layers [5]. The increase and decrease of roughness with changing laser energy may be due to the increased or reduced number of oxygen functional layers, respectively.

4. X-Ray Diffraction Analysis (XRD)

XRD analysis represented a very useful characterization tool that is used to study the physical properties, the crystallographic structure and chemical composition of materials and thin films [3]. Figure-5 shows the structural properties of GO and rGO as characterized using XRD analysis.

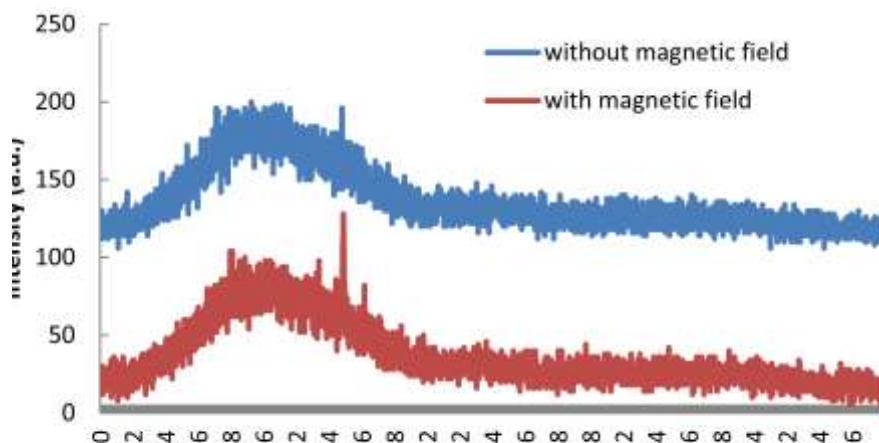


Figure 5-XRD patterns of GO prepared by laser at laser energy of 600mJ.

Figure-5 demonstrates the XRD data of GO prepared by laser with an energy of 600 mJ, with and without magnetic field. The XRD pattern of GO shows the broad peak observed at 2θ in the range

from 20-27° (20.5113°, 22.0972°, 22.9752°, 24.4721° and 26.4984°), with and without of the magnetic field. The 2θ peak in the range 20-26° corresponds to the interlayer distance (d space distance) of ~ 0.4 nm that may be resulting from formation of few graphene oxide (rGO) layers. This interlayer distance indicates the removal of oxygen functional groups [2]. By using Scherrer equation, the crystallite size (C) was calculated as [22]:

$$C = \frac{0.9 \times \lambda}{\beta \times \cos\theta} \dots \dots \dots (1)$$

where θ is the diffraction angle, β is the line width at half height in the radians, and λ is the cu kα wavelength (0.15418nm). According to equation (1), the crystallite size was calculated and shown in Table-2.

Table 2-Data obtained from XRD of GO without magnetic field at laser energy of 600 mJ.

2θ	d (nm)	FWHM	Crystallite Size (nm)
20.5113	0.432654	0.62	13.03
22.0972	0.401948	0.92	8.8
22.9752	0.386783	0.76	10.67
24.4721	0.363452	0.76	10.7
26.4984	0.336101	0.46	17.75

According to the results in table (2), the average crystallite size was equal to 12.19nm. While in the presence of magnetic field, the XRD shows the disappearance of the broad peak of the range 20-26° and the appearance of new peaks at 2θ in 26.5496, 31.7259 and 64.981°. The corresponding internal distance and crystallite size of these peaks are tabulated in Table-3.

Table 3-Data obtained from XRD of GO with magnetic field at laser energy of 600mJ.

2θ	d (nm)	FWHM	Crystallite Size (nm)
26.5496	0.335465	0.1493	54.71
31.7259	0.281813	0.1345	61.44
64.981	0.143402	0.0967	97.462

One can observe from Table-3 that the interlayer distance was decreased when the magnetic field was applied (approximately ~ 0.25nm). While the crystallite size was increased when the magnetic field was applied. This behavior may be attributed to the reduction of oxygen functional groups, which indicates the formation of rGO layers, with and without the magnetic field [22].

5. Fourier Transform Infrared Spectroscopy (FTIR)

The FTIR spectrum of GO demonstrated in Figure-6, when the magnetic field is not applied, at laser energy of 500mJ shows a broad peak in the high frequency region between 3000 –3700cm⁻¹ together with a sharp peak at 1627.81cm⁻¹ corresponding to the stretching and bending vibration of OH groups of water molecules adsorbed on graphene oxide [22-24]. Based on these results, it can be concluded that the sample has strong hydrophilicity. The peaks corresponding to 2921.96cm⁻¹ and 2856.38cm⁻¹ represent the symmetric and anti-symmetric stretching vibrations of CH₂ [2,4,6], while the absorption peak at 2354.92 cm⁻¹ can be attributed to the stretching vibration of C=O of carboxyl group [2]. The stretching vibration of C=C double bond of graphene appears at 1641cm⁻¹ [22, 23, 25]. The two absorption peaks at 1427.23cm⁻¹ and 1444.58cm⁻¹ correspond to the axial deformation of the C = C bonds [5]. The two absorption peaks at 1110.92cm⁻¹ and 1035.7cm⁻¹ correspond to the stretching vibration of C-O [7,26]. The O-H deformation is exhibited at the peaks range 1300 – 1400cm⁻¹ [2].When the laser energy was increased, FTIR spectrum showed that all absorption peaks were reduced and shifted toward the longest wavenumber. The reduction of peak intensities implies a successful reduction of the GO by using the laser beam [3].

Furthermore,, Figure-7 shows the FTIR spectra of GO at different laser energy levels in the presence of the magnetic field. The spectrum reveals absorption peaks between 300-3700cm⁻¹ together with a sharp peak at 1623.95cm⁻¹ which is attributed to the stretching and bending vibrations of OH groups of water molecules adsorbed on GO [22-24]. The two peaks at 2802.38cm⁻¹ and 2927.74cm⁻¹ correspond to the symmetric and anti-symmetric stretching vibrations of CH₂ [2, 4, 6]. The peak at 2366.49cm⁻¹ corresponds to the stretching vibration of C=O of carboxyl group [2]. The stretching vibration of C=C double bond of graphene appears at 16439.38cm⁻¹ [22, 23, 25]. The two absorption

peaks at 1267.14 and 1386.72 cm^{-1} are due to O-H deformation [2]. The axial deformation of the C = C bonds appears at 1429.15 cm^{-1} [5]. The absorption peaks appearing at 1031.85 cm^{-1} and 1105.14 cm^{-1} are due to the stretching vibration of C-O [7, 26]. When the laser energy was increased, the FTIR spectrum showed that the peaks that appeared in the spectra were reduced and shifted toward smallest wavelengths, while the stretching vibration of OH group was shifted to the lower wavenumber. Therefore, because not all oxygen functional groups were removed, the material was called reduced graphene oxide (rGO).

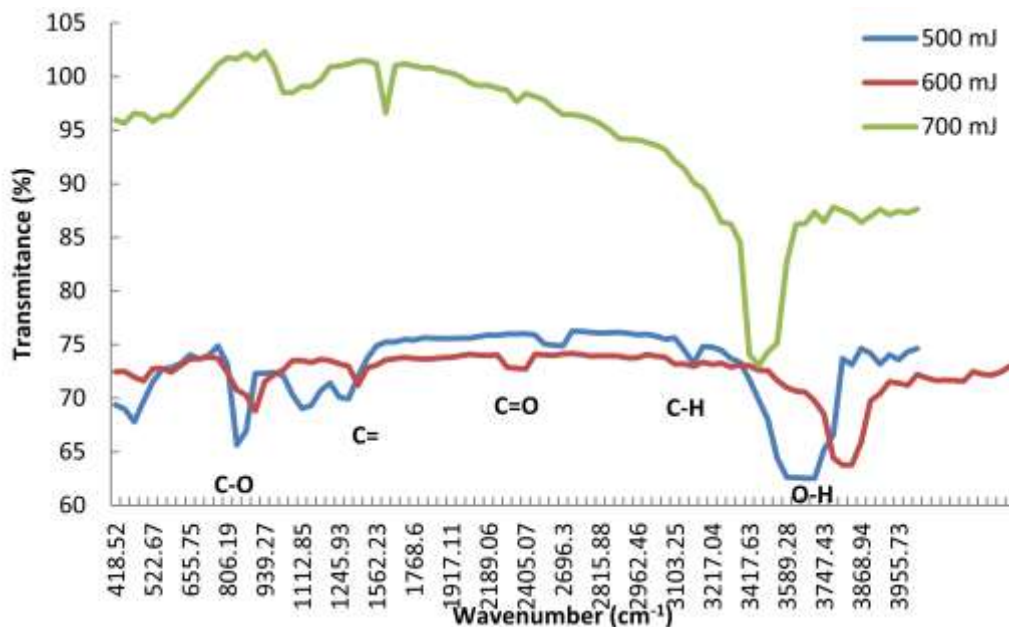


Figure 6-FTIR spectra of graphene oxide prepared at different laser energy in the absence of magnetic field.

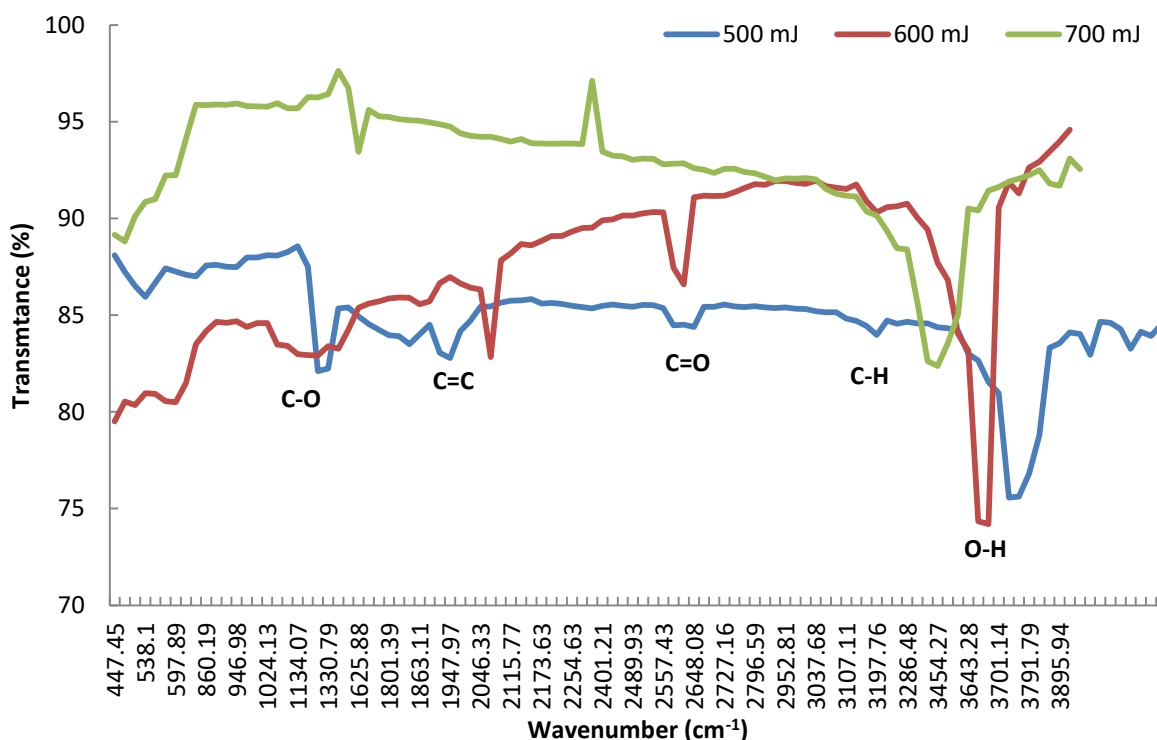


Figure 7-FTIR spectra of graphene oxide that prepared at different laser energy when the magnetic field was applied.

6. Conclusions

By using pure graphite as a laser target in laser ablation system, GO nanoparticles were successfully synthesized with and without magnetic field in this work. The synthesized GO nanoparticles were characterized by using several methods. The results of absorption spectrum of GO showed that the presence of magnetic field caused shifts in the absorption peaks toward longer wavelengths. However, in the absence of magnetic field, the absorption peaks were shifted toward lower wavelengths when the laser energy was increased from 500 to 600mJ, whereas there was no shift in the absorption peak when the laser energy became 700mJ. In addition, the peak intensity was increased when the laser energy was increased from 500 to 600mJ. But the intensity of the peak was decreased dramatically when the laser energy was increased to 700mJ. While in the presence of magnetic field, the absorption peaks were shifted toward longer wavelengths and the intensity of the peaks was increased with increasing laser energy. These results may be attributed to the increase of oxygen functional groups of GO in the presence of the magnetic field. The size and morphology of GO nanoparticles were characterized by AFM and suggested that the presence of magnetic field causes changes in the morphology of the surface and roughness average of GO nanoparticles. While the average diameter of GO nanoparticles was not affected by the applied magnetic field. The elemental GO in the presence and absence of magnetic field was confirmed through XRD which showed that when the magnetic field was applied, the crystallite size was increased while the interlayer distance (d-space) was reduced. This result indicates the successful penetration of oxygen functional groups between the layers. Finally, the interaction between distilled water and graphene nanoparticles was analyzed by FTIR which revealed that when the magnetic field was applied, the absorption peaks that appear in the spectrum were reduced and shifted toward smallest wavelengths, while the stretching vibration of the O-H group peak was shifted toward largest wavelength. This result implies that the presence of magnetic field has a good effect on the structure of graphene oxide.

References

1. Paulchamy, G. and Lignesh, D.B. **2015**. "A Simple Approach to Stepwise Synthesis of Graphene Oxide Nanomaterial", *Journal of Nanomedicine & Nanotechnology*, **6**(1): 1-4.
2. Ali Moosa and Noori Jaafar, J. **2017**. "Green Reduction of Graphene Oxide Using Tea Leaves Extract with Applications to Lead Ions Removal from Water", *Nanoscience and Nanotechnology*, **7**(2): 38-47.
3. Calinai, M. Demeter, E. Badita, E. Stancu, A. Scarisoreani and Vancea, C. **2017**. "Reduction of Freestanding Graphene Oxide Films Using Continuous Wave Laser", *Romanian Reports in Physics*, **69**(504): 1-7.
4. Mageed, K., Dayang Radiah, A.B., A. Salmiaton, A., Shamsul Izhar, M. Abdul Razak, H.M. Yusoff, F.M. Yasin, S. Kamarudin and Buthainah, A. **2016**. "Preparation and Characterization of Nitrogen Doped Reduced Graphene Oxide Sheet", *International Journal of Applied Chemistry*, **12**(1): 104-108.
5. Rodbari, R.J., Wendelbo, R., Jamshidi, L.C., Hernandez, E.P. and Nascimento, L. **2016**. "Study of Physical and Chemical Characterization of Nanocomposite Polystyrene/ Graphene Oxide High Acidity can be Applied in Thin Films", *J. Chil. Chem. Soc.*, **61**(3): 3120-3124.
6. Monteserín, M. Blanco, E. Aranzabe, A. Aranzabe, J. Manuel Laza, A. Larrañaga-Varga and J. Luis Vilas, **2017**. "Effects of Graphene Oxide and Chemically-Reduced Graphene Oxide on the Dynamic Mechanical Properties of Epoxy Amine Composites", *Polymers*, **9**(449): 1-16.
- a. Gharib, L. Vojdani Fard, N. Noroozi Pesyan and M. Roshani, **2015**. "A New Application of Nano-Graphene Oxide (NGO) as a Heterogeneous Catalyst in Oxidation of Alcohols Types", *Chemistry Journal*, **1**(4): 151-158.
7. M. J. McAllister, J. L. Li, D. H. Adamson, H. C. Schniepp, A. A. Abdala, J. Liu, M. H. Alonso, D. L. Milius, R. Car, R. K. Prudhomme, and I. A. Aksay, **2007**. "Single Sheet Functionalized Graphene by Oxidation and Thermal Expansion of Graphite" *Chem. Mater.*, **19**: 4396-4404.
8. Ambrosi, and Pumera, M. **2013**. "Precise Tuning of Surface Composition and Electron-Transfer Properties of Graphene Oxide Films Through Electro Reduction", *Chemistry—A European Journal*, **19**(15): 4748-4753.

9. Stankovich, S., Dikin, D.A., Piner, R.D., Kohlhaas, K.A., A. Kleinhammes, Y. Jia, Y. Wu, S.T. Nguyen and R. S. Ruoff, R. **2007**. "Synthesis of Graphene-Based Nano Sheets via Chemical Reduction of Exfoliated Graphite Oxide", *Carbon*, **45**: 1558–1565.
10. Bykkam, S., Venkateswara, R.K., Shilpa, C. and Thunugunta, T. **2013**. "Synthesis and Characterization of Graphene Oxide and Its Antimicrobial Activity Against *Klebsiella* and *Staphylococcus*", *International Journal of Advanced Biotechnology and Research*, **4**(1): 142-146.
11. Lerf, H., He, Y., Forster, M. and Klinowski, J. **1998**. "Structure of graphite oxide revisited", *J Phys Chem B*, **102**: 4477-4482.
12. Wang X, Zhi L. and k. Mullen, K. **2007**. "Transparent, conductive graphene electrodes for dye-sensitized solar cells", *Nano Lett*, **8**: 323-327.
13. Dikin, A., Stankovich, S., Zimney, E.J., Piner, R.D., Dommett, G.H., Evmenenko, G., Nguyen, S.T. and Ruoff, R.S. **2007**. "Preparation and characterization of graphene oxide paper", *Nature* **448**: 457-460.
14. Liang, J., J., Y. Xu, J.Y., Y., D. Sui, Y.D., D., L. Zhang, D.L., Y. Huang, Y., Y. Ma, Y., F. Li, F., Y. Chen, Y. **2010**. "Flexible, magnetic and electrically conductive graphene/ Fe_3O_4 Paper and its application for magnetic controlled switches", *J Phys Chem C*, **1141**: 17465-174771.
15. Bunch, J.S., van der Zande, A.M., Verbridge, S.S., Frank, I.W., Tanenbaum, D.M., Parpia, J.M., Craighead, H.G. and McEuen, P.L. **2007**. "Electromechanical Resonators from Graphene", *Science*, **315**: 490, 2007.
16. Eda, G. and Chhowalla, M. **2009**. "Graphene-based Composite Thin Films for Electronics", *Nano Lett*, **9**: 814-818.
17. Mohanty, N. and Berry, V. **2008**. "Graphene-based singal-bacterium resolution biodevice and DNA transistor: Interfacing graphene derivative with nanoscale and microscale biocomponents", *Nano Lett*, **8**: 4469-4476.
18. Morales-Narváez and A. Merkoçi, **2012**. "Graphene oxide as an optical biosensing platform," *Adv. Mater.*, **24**(25): 3298–3308.
19. Yeh, T.F., Cihlar, J., Chang, C.Y., Cheng, C. and H. Teng, H. **2013**. "Roles of graphene oxide in photocatalytic water splitting," *Mater. Today*, **16**(3): 78–84.
20. Eda, G. and Chhowalla, M. **2010**. "Chemically derived graphene oxide: Towards large-area thin-film electronics and optoelectronics," *Adv. Mater.*, **22**(22): 2392–2415.
21. G. Pavoski, G., T. Maraschin, T., F. de Carvalho Fim, F., N. Maria Balzaretta, N., G. Barrera Galland, G., Cássio Stein M. and Nara Regina de Souza B. **2017**. "Few Layer Reduced Graphene Oxide: Evaluation of the Best Experimental Conditions for Easy Production", *Materials Research*, **20**(1): 53-61.
22. Ban, F.Y. Majid, S.R. Huang, N.M. and Lim, H.N. **2012**. "Graphene Oxide and Its Electrochemical Performance", *Int. J. Electrochem. Sci.*, **7**: 4345 – 4351.
23. Kravets, V.G., Marshall, O.P., Nair, R.R., Thackray, B., Zhukov, A., Leng, J. and Grigorenko, A.N. **2015**. "Engineering optical properties of a graphene oxide metamaterial assembled in microfluidic channels", *Optical Society of America*, **23**(2): 1265-1275.
24. Khan, M., Al-Marri1, A.H., Khan, M., Rafi Shaik, M., Mohri, N., Farooq Adil, S., Kuniyil, M., Alkathlan, H.Z., Al-Warthan, A., Tremel, W., Nawaz Tahir, M. and Rafiq M., Siddiqui, H. **2015**. "Green Approach for the Effective Reduction of Graphene Oxide Using *Salvadora persica* L. Root (Miswak) Extract", *Nanoscale Research Letters*, **10**(281): 1-9.
25. Nithya, M. **2015**. "Electrochemical Sensing of Ascorbic Acid on ZnO-decorated Reduced Graphene Oxide Electrode", *Journal of Biosensors & Bioelectronics*, **6**(1): 1-9